Cell adaptation to aneuploidy by the environmental stress response dampens induction of the cytosolic unfolded-protein response

Andrew J. Kane[a,†], Christopher M. Brennan[b,c,d,†,‡], Acer E. Xu[b,c,d], Eric J. Solís[a], Allegra Terhorst[b,c,d], Vladimir Denic[a,*], and Angelika Amon[b,c,d]

[a]Department of Molecular and Cellular Biology, Harvard University, Cambridge, MA 02138; [b]David H. Koch Institute for Integrative Cancer Research, [c]Howard Hughes Medical Institute, and [d]Paul F. Glenn Center for Biology of Aging Research, Massachusetts Institute of Technology, Cambridge, MA 02139

ABSTRACT **Aneuploid yeast cells are in a chronic state of proteotoxicity, yet do not constitutively induce the cytosolic unfolded protein response, or heat shock response (HSR) by heat shock factor 1 (Hsf1). Here, we demonstrate that an active environmental stress response (ESR), a hallmark of aneuploidy across different models, suppresses Hsf1 induction in models of single-chromosome gain. Furthermore, engineered activation of the ESR in the absence of stress was sufficient to suppress Hsf1 activation in euploid cells by subsequent heat shock while increasing thermotolerance and blocking formation of heat-induced protein aggregates. Suppression of the ESR in aneuploid cells resulted in longer cell doubling times and decreased viability in the presence of additional proteotoxicity. Last, we show that in euploids, Hsf1 induction by heat shock is curbed by the ESR. Strikingly, we found a similar relationship between the ESR and the HSR using an inducible model of aneuploidy. Our work explains a long-standing paradox in the field and provides new insights into conserved mechanisms of proteostasis with potential relevance to cancers associated with aneuploidy.**

Monitoring Editor
Elizabeth Miller
MRC Laboratory of Molecular Biology

Received: Mar 8, 2021
Revised: Jun 17, 2021
Accepted: Jun 21, 2021

INTRODUCTION

Errors in chromosome segregation during mitosis result in aneuploid cells carrying an incorrect number of chromosomes. Thus, aneuploidy is associated with decreased cellular fitness, developmental defects, and cancer. Because genes on autosomes are expressed according to their genetic copy number, aneuploid cells have imbalanced proteomes (Torres *et al.*, 2007, 2010; Pavelka *et al.*, 2010; Dephoure *et al.*, 2014). These stoichiometric imbalances of protein complexes lead to protein misfolding and aggregation (Brennan *et al.*, 2019), generating stress on the cellular protein-folding and -degradation machinery (Torres *et al.*, 2007, 2010; Oromendia *et al.*, 2012; Donnelly *et al.*, 2014; Santaguida *et al.*, 2015). Despite a large body of evidence that aneuploidy is proteotoxic, how protein homeostasis (proteostasis) mechanisms respond to aneuploidy still remains poorly understood.

In eukaryotic cells, cytosolic protein misfolding induces a transcriptional up-regulation of chaperones known as the cytosolic unfolded protein response (HSR) (Trotter *et al.*, 2002; Dobson, 2003; Geiler-Samerotte *et al.*, 2011; Hartl *et al.*, 2011). In budding yeast, heat shock factor 1 (Hsf1) is an essential and conserved transcription factor mediating the HSR. A recent study demonstrated that Hsf1 and cytosolic Hsp70 chaperones enable a negative-feedback mechanism whereby elevated levels of unfolded proteins during

This article was published online ahead of print in MBoC in Press (http://www.molbiolcell.org/cgi/doi/10.1091/mbc.E21-03-0104) on June 30, 2021.

†These authors contributed equally to this work.

‡Present address: Rare Disease Research Unit, Pfizer, Cambridge, MA 02139

Author contributions: A.J.K., C.M.B., A.J.K., A.E.X, E.J.S, A.T., A.A., and V.D. performed experiments and analyzed results; A.J.K., C.M.B., A.E.X, E.J.S, A.T., A.A., and V.D wrote the manuscript; A.J.K., C.M.B., A.E.X, E.J.S, A.T., and V.D read and approved the final manuscript.

*Address correspondence to: Vladimir Denic (vdenic@mcb.harvard.edu).

Abbreviations used: ESR, environmental stress response; HDG, Hsf1 dependent gene; HSR, heat shock response; IAA, 3-indoleacetic acid; PKA, protein kinase A.

folding stress titrate Hsp70 from binding to Hsf1 as a repressor (Zheng *et al.*, 2016; Krakowiak *et al.*, 2018). Proteostasis is restored following Hsf1 induction when sufficient amounts of Hsp70 bind to and down-regulate Hsf1. Besides promoting Hsp70 expression, Hsf1's essential role in the cell is to control a small number of Hsf1-dependent genes (HDGs) comprising mostly protein folding factors (Solís *et al.*, 2016).

Despite the clear association of aneuploidy with proteotoxicity, there is no evidence of HSR induction in aneuploid cells (Oromendia *et al.*, 2012). A potential issue is that analysis of aneuploid stress responses has mostly been conducted on cells with single-chromosome gain. It is possible that higher levels of chromosomal imbalance are necessary to induce the HSR. Further complicating matters is that aneuploid cells have transcriptional signatures of the environmental stress response (ESR; Gasch *et al.*, 2000; Torres *et al.*, 2007). The yeast ESR is characterized by transcriptional activation of ~300 genes and repression of ~600 genes (Gasch *et al.*, 2000) in response to diverse exogenous stressors and mutations that confer slow growth (Brauer *et al.*, 2008). Protein kinase A (PKA) is a master regulator of the ESR that is repressed during stress by binding to its regulatory subunit Bcy1 (Santangelo, 2006). This leads to dephosphorylation and activation of Msn2/4, a pair of transcription factors that regulate the expression of most genes associated with the ESR (Görner *et al.*, 1998). Interestingly, the expression of certain chaperones is up-regulated by Msn2/4, raising the possibility of negative cross-talk between the ESR and Hsf1 during aneuploidy (Gasch *et al.*, 2000; Solís *et al.*, 2016).

Here we examine how PKA activity affects proteostasis in aneuploid cells and during heat stress in euploids. These complementary systems enable us to propose a unifying model in which the ESR down-regulates the HSR in response to stress while protecting cells from proteotoxicity.

RESULTS

The environmental stress response suppresses cytosolic unfolded-protein response induction in aneuploid cells and heat shock

The transcriptional state of aneuploid cells resembles the ESR, a generic response to a wide variety of different stressors, including heat shock (Gasch *et al.*, 2000; Torres *et al.*, 2007). Intriguingly, yeast gene deletions that result in an elevated ESR also have a dampened HSR (Brandman *et al.*, 2012), similar to the state of these responses in aneuploid cells (Oromendia *et al.*, 2012). Thus, we hypothesized that suppressing the ESR should uncover a latent HSR in aneuploid cells. To test this, we engineered activation of PKA, a master kinase that represses ESR activation, using an auxin-inducible degradation (AID) allele of Bcy1, which encodes the repressing subunit of PKA (Santangelo, 2006). This system enabled rapid depletion of Bcy1 within 1 h of auxin (3-indoleacetic acid) addition (Figure 1A) and inhibited growth on a nonfermentable carbon source (Supplemental Figure S1A), as expected for cells with constitutively active PKA (Kunkel *et al.*, 2019). To monitor the HSR, we used qRT-PCR to analyze expression of an HDG, *BTN2* (Solís *et al.*, 2016), which encodes a chaperone involved in misfolded protein sequestration. In a control experiment using wild-type cells, *BTN2* became highly induced within 15 min of shifting cells to 39°C but rapidly returned to its preinduced state despite persistent heat stress (Figure 1B). Consistent with our hypothesis, depletion of Bcy1 in a panel of disomic (VIII, XIV, and XV) yeast strains uncovered significant *BTN2* induction (Figure 1, C–E; Supplemental Figure S1B) in proportion to the size of the extra chromosome.

In an orthogonal approach, we showed that the ESR is sufficient to suppress the HSR. Specifically, we used a strain in which all three alleles of the catalytic PKA subunits (TPK1/2/3) are sensitive to the ATP analog 1-NM-PP1 (*as-TPK1/2/3*; Bishop *et al.*, 2000; Yorimitsu *et al.*, 2007). Pretreatment of *as-TPK1/2/3* with 1-NM-PP1 robustly suppressed *BTN2* induction by subsequent heat shock at 39°C, while having no effect on cells with wild-type TPK alleles (*wt-TPK1/2/3*; Figure 1F and Supplemental Figure S1C). We note that the relatively low basal expression of *BTN2* as an HDG makes it a sensitive reporter of Hsf1 activity but can also lead to variability in absolute *BTN2* induction between experiments. Importantly, this readout of the HSR consistently captured differences between strains and treatment conditions throughout our study.

The environmental stress response is cytoprotective against proteotoxicity

The ESR is considered an adaptive cell response, but its role in aneuploidy has not been fully explored. Thus, we looked for potential synthetic growth defects of Bcy1p depletion on the proliferation of a panel of disomic (VIII, XIV, and XV) yeast strains in the presence of two kinds of proteotoxicity. First, we used AZC, an amino acid analog that causes widespread protein misfolding (Trotter *et al.*, 2001). While we observed a trend in synthetic growth defects that increased with the size of the extra chromosome, none were statistically significant (Supplemental Figure S2, A–C). Notably, we could detect a robust synthetic growth defect at the semipermissive temperature of *ndc10-1* (Figure 2A). This temperature-sensitive mutant has a relatively severe form of aneuploidy in which it missegregates ~60% of chromosomes after being shifted to its semipermissive temperature of 34°C (Oromendia *et al.*, 2012). Next, we looked for synthetic growth defects at 37°C and found that cells carrying the smallest of the three duplicated chromosomes tested (VIII) grew comparably to the euploid control strain (Figure 2B). However, disomy of larger chromosomes (XIV and XV) resulted in a clear synthetic loss in viability (Figure 2B). Together, these data reveal that the ESR confers cytoprotection against proteotoxicity in aneuploids commensurate with their proteomic imbalance, ranging from high (*ndc10-1*) to intermediate (XV/XIV disomes) to low (VIII disomy).

In an orthogonal approach, we demonstrated that the ESR is sufficient to protect euploid cells from proteotoxicity due to heat stress. First, pretreatment of *as-TPK1/2/3* but not control *wt-TPK1/2/3* cells with 1-NM-PP1 conferred robust protection from severe heat stress (50°C; Coote *et al.*, 1994; Figure 2C). Second, we monitored the effect of ESR on heat-induced protein aggregation using Hsp104 localization. Fluorescently tagged Hsp104 rapidly becomes targeted to visible puncta of protein aggregates following heat shock at 39°C (Grimminger-Marquardt and Lashuel, 2010). Quantitative image analysis confirmed that only mock treatment of *as-TPK1/2/3* cells led to the expected increase in Hsp104-marked aggregates at 39°C, whereas pretreatment with 1-NM-PP1 prevented all protein aggregation (Figure 2, D and E).

Cytosolic unfolded-protein response inactivation during persistent heat shock is driven by the environmental stress response

To extend these observations beyond aneuploidy, we examined the relationship between the HSR and the ESR during heat shock. As our readout of the ESR, we relied on qRT-PCR analysis of *HSP26*. This canonical target of the ESR (Gasch *et al.*, 2000) was induced during the first 20 min of heat shock before returning to

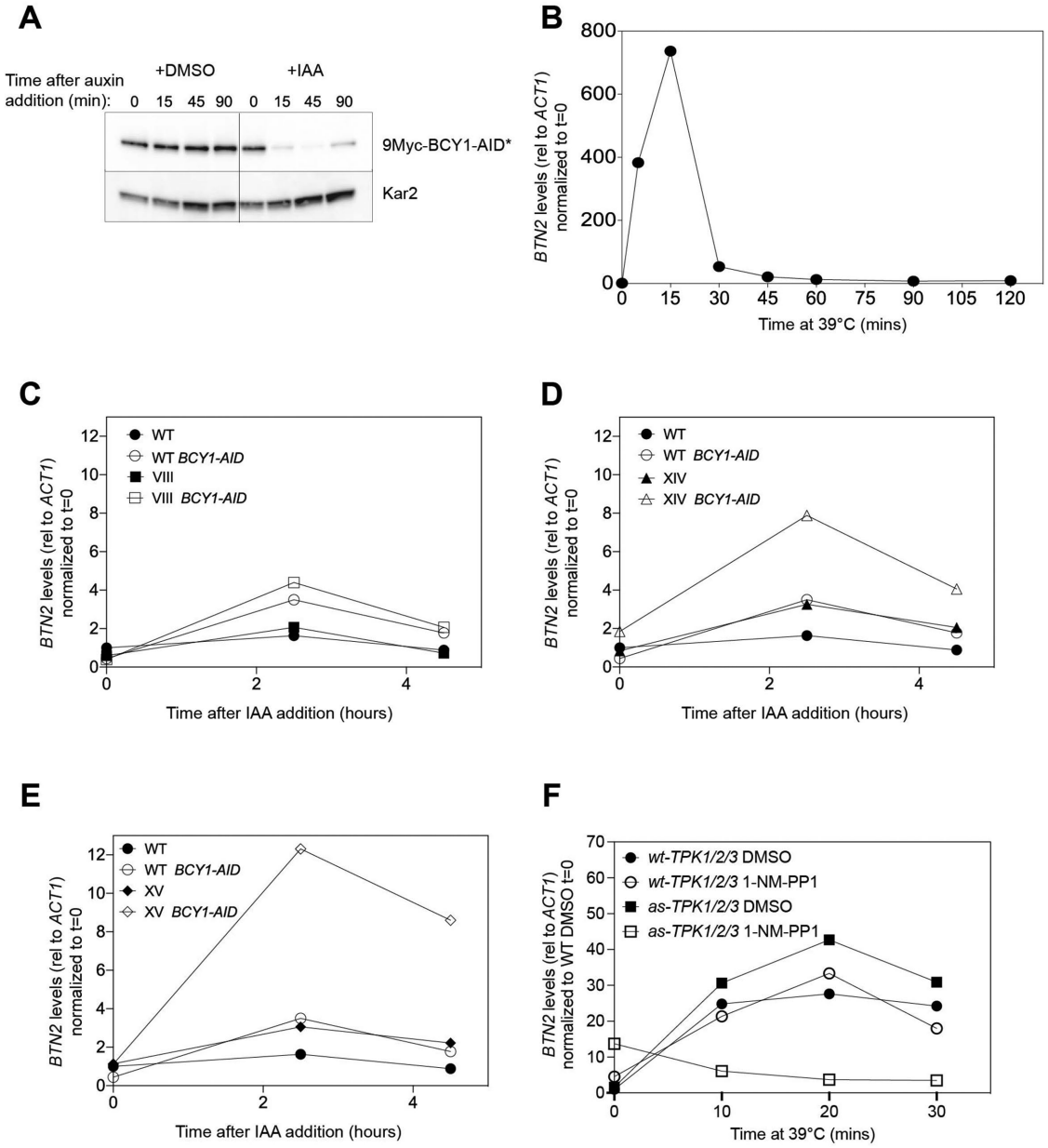

FIGURE 1: Hsf1 induction by aneuploidy and heat stress is suppressed by the ESR. (A) *BCY1-AID* (A40439) cells were grown exponentially at 30°C in YEP-D. Following removal of the 0′ timepoint for analysis, auxin was added to each culture and samples were removed at the indicated timepoints. Bcy1 levels were measured by Western blot ($n = 1$). (B) WT (A2587) cells were grown exponentially at 30°C in YEP-D. Following removal of the 0′ timepoint, cells were shifted to 39°C and additional samples removed at the indicated timepoints. *BTN2* mRNA levels in each sample were determined by qRT-PCR. Shown is a plot of all the measurements first normalized to *ACT1* levels and then to $t = 0'$ ($n = 1$). (C—E) WT (A2587), *BCY1-AID* (A40439), Dis VIII (A15533), Dis VIII; *BCY1-AID* (A40962), Dis XIV (A15540), Dis XIV; *BCY1-AID* (A40964), Dis XV (A15542), and Dis XV. *BCY1-AID* (A40861) cells were grown exponentially at 30°C in YEP-D. Following removal of the 0′ timepoint for analysis, auxin was added to each culture and additional samples were removed at the indicated timepoints. *BTN2* mRNA levels of each sample were determined as in B. Shown are representative samples of two biological replicates for Dis XV ($n = 1$). (F) WT (VDY465) and *as-TPK1/2/3* (VDY466) cells were grown exponentially at 30°C in YEP-D and pretreated with 1-NM-PP1 or mock treated with carrier (DMSO) for 3 h at 30°C. Following removal of the 0′ timepoint, cells were shifted to 39°C and additional samples removed at the indicated timepoints. *BTN2* mRNA levels of each sample were determined as in B. Shown is a representative sample of two biological replicates ($n = 1$). Abbreviations: rel = relative, mins = minutes.

its pre-induced state (Supplemental Figure S3, A and B). Importantly, depletion of Bcy1 before heat shock suppressed *HSP26* induction (Supplemental Figure S3, C and D) while resulting in prolonged *BTN2* induction (Figure 3 and Supplemental Figure S3E), as well as induction of two other Hsf1 gene targets (Supplemental Figure S3, F and G). Collectively, these data demonstrate that the ESR also curbs Hsf1 activity during heat shock in euploid cells.

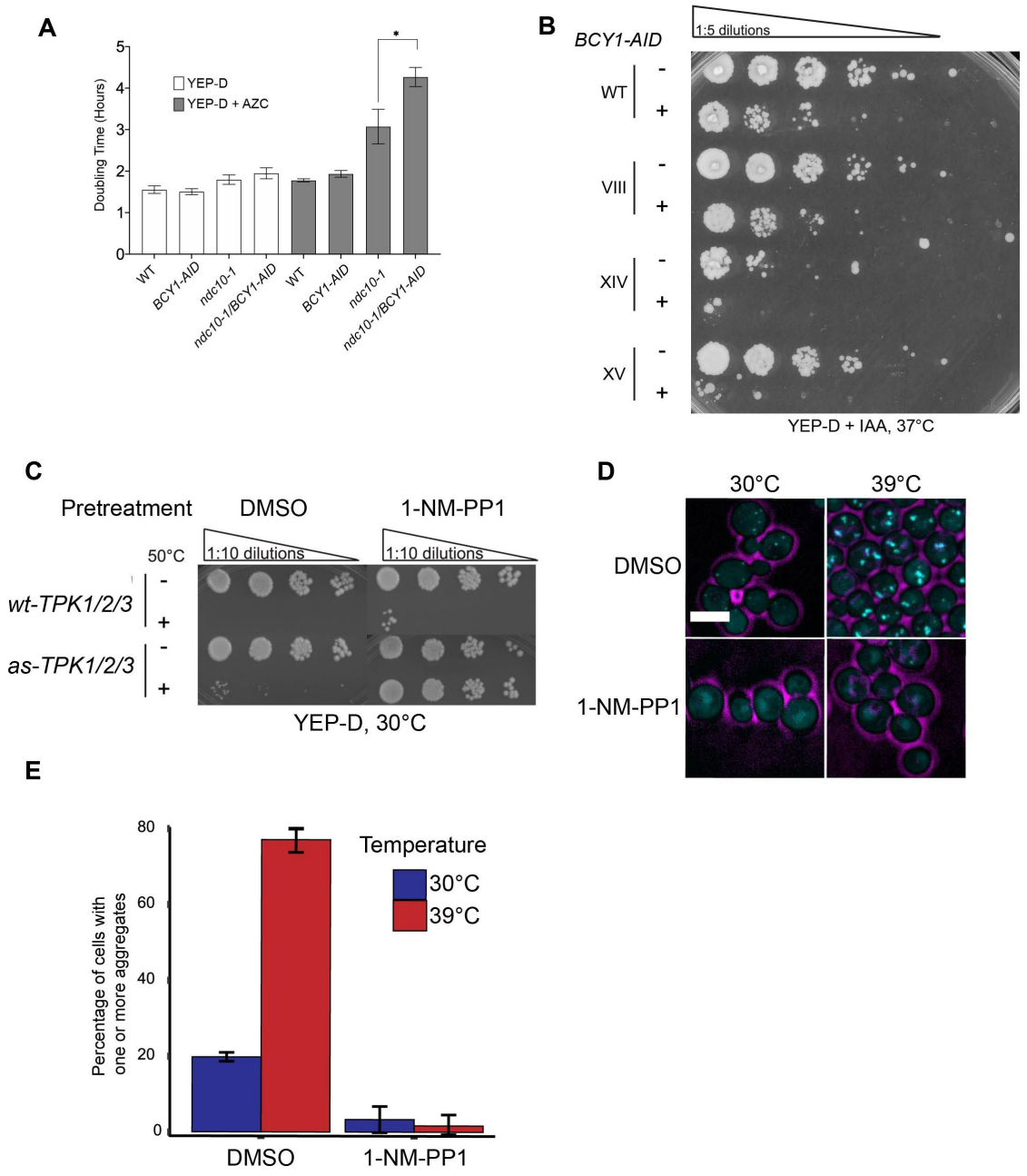

FIGURE 2: Evidence that the ESR protects euploid and aneuploid cells from proteotoxicity. (A) WT (A16629), *BCY1-AID* (A1012), *BCY-AID* (A40775), and *ndc10-1*. BCY1-AID (A40852) cells were grown exponentially in YEP-D before being treated with auxin for 1 h. Following a shift to 32°C, the doubling time of AZC or mock-treated cells was determined by OD_{600}. Data shown are the average of three biological replicates ($n = 3$). Error bars represent SD from the mean of experimental replicates. A Student's *t* test was performed on AZC treated *ndc10-1* cells. $p < 0.05$. (B) WT (A2587), *BCY1-AID* (A40439), Dis VIII (A15533), Dis VIII; *BCY1-AID* (A40962), Dis XIV (A15540), Dis XIV; *BCY1-AID* (A40964), Dis XV (A15542), and Dis XV. *BCY1-AID* (A40861) cells were grown exponentially at 30°C in YEP-D and pretreated with auxin for 1 h before spotting onto a YEP-D plate containing auxin. Each culture was normalized to the same OD_{600} and spotted as part of a fivefold dilution series. Shown is a representative plate image after incubation at 37°C for 2 d ($n = 1$). (C) *wt-TPK1/2/3* (VDY465) and *as-TPK1/2/3* (VDY466) cells were grown exponentially in YEP-D at 30°C and pretreated with 1-NM-PP1 or mock treated with carrier (DMSO) for 3 h. Cells were then exposed to 50°C for 30 min (+) or left on ice (-) before spotting onto solid YEP-D. Each culture was normalized to the same OD_{600} and plate spotted in a 10-fold dilution series. Shown is a representative plate image after 2 d of incubation ($n = 2$). (D) *as-TPK1/2/3* cells expressing GFP-tagged Hsp104 (VDY3647) were grown exponentially in SDC at 30°C and pretreated with 1-NM-PP1 or mock treated with carrier (DMSO) for 3 h. Each sample was split and diluted 1:2 with fresh media prewarmed to either 30 or 50°C to induce a rapid 39°C heat shock in the latter, and incubated further for 1 h at 30°C or 39°C, respectively. Samples were analyzed by confocal microscopy. Shown are representative micrographs of Hsp104-GFP localization (cyan; cell outlines in magenta) of three fields of view ($n = 3$). Scale bar represents 5 μm. (E) Percentage of cells with one or more aggregates imaged in D ($n = 3$).

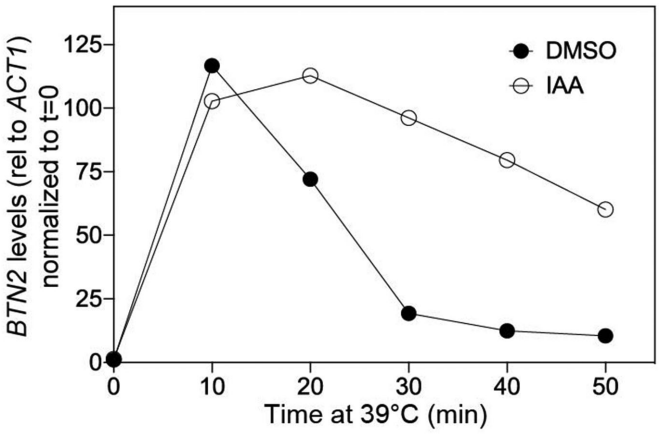

FIGURE 3: ESR quenches Hsf1 activity during heat shock. *BCY1-AID* (A40439) cells were grown exponentially in YEP-D at 30°C before being pretreated with auxin (IAA) or mock treated with carrier (DMSO) for 1 h. Following removal of the 0′ timepoint, cells were shifted to 39°C and additional samples removed at the indicated timepoints. *BTN2* mRNA levels of each sample were determined as in Figure 1B. Shown is a representative sample of two biological replicates ($n = 1$). Abbreviations: rel = relative, mins = minutes.

The environmental stress response suppresses the cytosolic unfolded protein response during induction of severe aneuploidy

Given the transient nature of Hsf1 induction during heat shock, we considered the possibility of similar dynamics during onset of aneuploidy in *ndc10-1* cells. As a control, we first monitored *BTN2* gene expression in WT cells following a temperature shift to 34°C and found only the expected transient induction during the first 30 min. In contrast, *ndc10-1* cells showed initially WT-like dynamics, but then *BTN2* levels began to increase again, starting at around 90 min, and continued for the remainder of the 150-min shift (Figure 4A and Supplemental Figure S4A). Importantly, Bcy1 depletion during this period resulted in further induction of *BTN2* in *ndc10-1* cells but not WT controls (Figure 4B and Supplemental Figures S4B).

DISCUSSION

Evidence suggests that aneuploidy causes proteotoxicity due to excess subunits of heteromeric protein complexes (Oromendia and Amon, 2014; Brennan *et al.*, 2019). Yet cells carrying even a relatively large single extra chromosome do not appear to have elevated Hsf1 activity (Oromendia *et al.*, 2012). We resolve this paradox by revealing that inhibition of the ESR in such a disomic background uncovers a latent Hsf1 stimulus. Notably, we were not able to uncover Hsf1 induction by disomes with smaller extra chromosomes. However, we found that aneuploidy induction in *ndc10-1* cells was sufficient to induce an HSR akin in magnitude to that from a mild heat shock at 34°C. It is worth noting that random chromosome missegregation under these conditions results in a heterogeneous population of aneuploid cells. Future studies of *ndc10-1* cells carrying markers for specific chromosomes (e.g. GFP dots; Straight *et al.*, 1996) and sensitive single-cell readouts of Hsf1 activity could deconvolve the contributions of individual chromosomes to HSR dynamics. For example, a recent study found that some strains of randomly generated aneuploid yeast containing an extra copy of chromosome II do not have an ESR or proteotoxic stress (Larrimore *et al.*, 2020). Consistent with this, disome II strains constructed by chromosome transfer were previously shown to have only a very mild proliferation defect and a transcriptional profile that closely resembled euploid strains (Torres *et al.*, 2007). We did not analyze strains disomic for chromosome II in this study, but it would be interesting to determine what chromosome II genes enable tolerance to proteostasis disruption by aneuploidy.

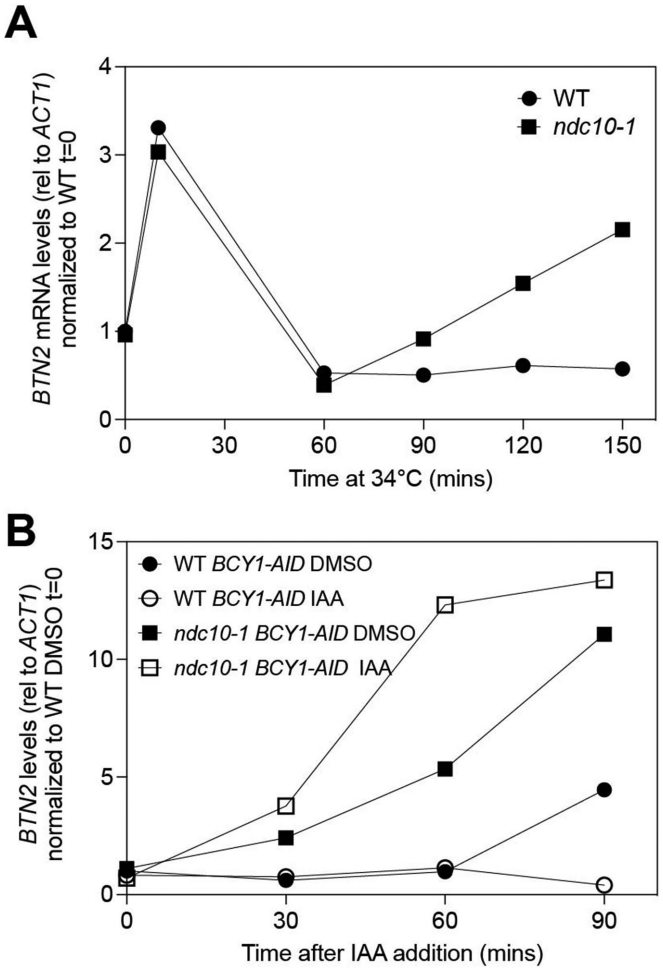

FIGURE 4: ESR quenches Hsf1 activity during aneuploidy induction. (A) WT (A2587) and *ndc10-1* (A40759) cells were grown exponentially in YEP-D at room temperature. Following removal of the 0′ timepoint, cells were shifted to 34°C. Subsequent time points were taken at the indicated times and *BTN2* levels were analyzed as in Figure 1B. Shown is a representative sample of two biological replicates ($n = 1$). (B) *BCY-AID* (A40439) and *ndc10-1*; BCY1-AID (A40761) cells were grown exponentially in YEP-D at room temperature. Cells were shifted to 34°C for 2 h. Following removal of the 0′ timepoint, cells were treated with auxin (IAA) or mock treated with carrier (DMSO) and additional samples were removed at the indicated timepoints. *BTN2* mRNA levels of each sample. Shown is a representative sample of two biological replicates ($n = 1$). Abbreviations: rel = relative, mins = minutes.

Activation of Hsf1 by heat shock has been a historical paradigm for transcriptional responses that restore proteostasis (Sorger and Pelham, 1987; Anckar and Sistonen, 2011). Recent work has shown, however, that while Hsf1's basal activity is essential for production of a small but critical subset of chaperones, the majority of transcriptional changes associated with heat shock are mediated by the ESR (Solís *et al.*, 2016). Here, we have shown that engineered activation of the ESR in the absence of heat stress leads to robust thermotolerance and precludes formation of heat-induced protein aggregates. Defining the mechanistic basis of these effects and their relationship

to Hsf1 attenuation by the ESR is an important future goal. We speculate on the involvement of Msn2 and Msn4, two transcription factors repressed by PKA that induce a variety of chaperone genes, most notably the disaggregase Hsp104 (Boy-Marcotte *et al.*, 1998; Grably *et al.*, 2002). Aneuploids may also be buffered against proteostasis collapse by the repressive effects of the ESR on protein synthesis, which normally imposes a large burden on protein folding in rapidly dividing cells. A better understanding of signaling mechanisms responsible for these observations (Crawford and Pavitt, 2018) is necessary for future testing of this otherwise attractive hypothesis.

Our work while restricted to yeast has potential relevance to human aneuploidy-associated cancers. One of the most frequently observed genomic alterations in cancer is the gain of the q arm of chromosome 8 (Beroukhim *et al.*, 2010; Davoli *et al.*, 2013). This region contains the oncogene Myc, which promotes cell proliferation by increasing biosynthetic pathways including protein synthesis (Hsieh *et al.*, 2015). In these types of cancer, cells appear to maintain proteostasis without sacrificing fitness, thanks to the presence of HSF1 on the same chromosome 8q arm (Dai *et al.*, 2007; Jin *et al.*, 2011). Specifically, these cancer cells are much more dependent on HSF1 activity for their proliferation and survival than untransformed cells. Thus, in certain oncogenic backgrounds, the essential role of HSF1 resembles that of Hsf1 in euploid yeast (Solís *et al.*, 2016). In contrast, aneuploid yeast cells seem to have supplanted Hsf1's basal role in proteostasis by inducing the ESR at the cost of reduced growth rate, a known effect of ESR signaling (Ho and Gasch, 2015). It remains to be determined whether evolving aneuploid yeast cells by selecting for clones with increased fitness will also lead to increased dependence on Hsf1.

MATERIALS AND METHODS

Yeast strains, plasmids, and growth conditions

All yeast strains are derivatives of W303 and are described in Table S1. Plasmids are listed in Table S2. Yeast strains were generated and manipulated as described previously (Guthrie and Fink, 1991). Cells were grown at indicated temperatures in YEP supplemented with 2% glucose (YEP-D). For microscopy and flow cytometry experiments, cells were grown in YEP-D or complete synthetic media with glucose (SDC, 0.67% yeast nitrogen base [BD Biosciences], 2% glucose, 1 × CSM [Sunrise Sciences, San Diego, CA]). Strains harboring temperature-sensitive mutations in *NDC10* were grown overnight at room temperature, back-diluted, and grown exponentially at room temperature before shifting to the semipermissive temperature of 34°C. For auxin treatments, cells were cultured in YEP-D containing 138 µl of glacial acetic acid per 1 l of medium, and auxin in the form of 3-indoleacetic acid (Sigma) was added to a final concentration of 500 µM. For 1-NM-PP1 treatments, cells were cultured in SDC and 1-NM-PP1 was added to a final concentration of 3 µM for 3 h.

Disomes used in this study are derivatives of those published in (Torres *et al.*, 2007). Gene deletions, fusion proteins, and promoter swaps were generated using PCR-based methods (Longtine *et al.*, 1998) in a wild-type W303 yeast strain. Disomes carrying gene manipulations were constructed by crosses.

Real-time qRT-PCR

Cells were grown as indicated and 0.2–2 OD_{600} units of culture were pelleted by centrifugation. The pellet was flash frozen in liquid nitrogen and stored at -80°C. To extract total RNA, ~200 µl of glass beads, 400 µl TES buffer (10 mM Tris pH 7.5, 10 mM EDTA, 0.5% SDS), and 400 µl of acid phenol:chloroform (pH 4.5) were added to the cell pellet, and the tubes were vortexed for 30 min at 65°C. The phases were separated by centrifugation, and the top phase was transferred to a new tube containing 1 ml of 120 mM sodium acetate in ethanol to precipitate RNA at 4°C. Precipitates were collected by centrifugation and resuspended in 100 µl of DEPC-treated water. Total RNA was further purified using the RNeasy Mini kit (Qiagen), including DNase treatment, according to the manufacturer's instructions. cDNA was synthesized from 750 ng of total RNA using the SuperScript III First-Strand Synthesis SuperMix kit (Invitrogen) with random hexamer primers according to the manufacturer's instructions. Real-time qRT-PCR reactions were run using the SYBR Premix Ex Taq Perfect Real Time kit (TaKaRa Bio) and a Roche LightCycler 480 (Roche) according to the manufacturer's instructions. qRT-PCR primers are as follows: BTN2 5′-GGCATCAACGAACCAAAGAT-3′ and 5′-GGCAGCTTTTTCCTGTTCTG-3′; ACT1 5′-GTACCACCATGTTCCCAGGTATT-3′ and 5′-CAAGATAGAACCACCAATCCAGA-3′ SSA1/2 5′-TGTCGCTCCATTATCCTTGGG-3′ and 5′-AGTGGAAAAGATCTCGGACTTC-3′.

BCY1 Western

Cells containing the BCY1-AID allele (A40439) were grown to OD_{600} = 0.1–0.2 at 25°C in YEP-D with added glacial acetic acid as described above. Auxin or DMSO was added, and cells continued to grow at 25°C. At each time point, 1 OD_{600} unit of culture was taken for immunoblot samples. Immunoblot samples were prepared as described in Weidberg and Amon (2018). A quantity of 20 µl of each sample was separated on a Novex 10% Tris-Glycine Mini Gel from Thermo Fisher, which was subsequently transferred to a nitrocellulose membrane (GE Life Sciences). The membrane was incubated with an anti-Myc antibody (1:1000 dilution; Sigma, 9E10). An anti-Kar2 antibody (1:200,000 dilution; gift from Mark Rose) was used as a loading control. Immunoblots were then treated with HRP-conjugated secondary antibodies (GE Healthcare) and ECL Western blotting detection reagents (Amersham) and then scanned on an ImageQuant LAS4000.

Microscopy

Cells were grown as during flow cytometry. Fixation was performed by rotating cells end over end for 15 min. Cells were pelleted by centrifugation, washed thrice with phosphate-buffered saline (PBS) 7.0, and resuspended in PBS 7.0 with 2 mM EDTA. To break up clumped cells caused by fixation, cells were sonicated for 30 s at 30% power on a Branson SFX 250 digital sonifier (Emerson Electric, St. Louis, MO). Fixed cells were applied directly to a well of concanavalin A (MP Biomedicals, Santa Ana, CA)-coated Lab-Tek II chambered cover glass (Thermo Fisher) and allowed to adhere for 5 min at room temperature. PBS was removed and cells were overlaid with 1% agarose pads containing PBS. Imaging was performed on a TI microscope (Nikon, Tokyo, Japan) equipped with a CSU-10 spinning disk (Yokogawa, Tokyo, Japan), an ImagEM EM-CCD camera (Hamamatsu, Hamamatsu, Japan), and a 100 × 1.45 NA objective (Nikon), equipped with 488-nm and 591-nm wavelength lasers (Coherent, Santa Clara, CA) and controlled with MetaMorph imaging software (Molecular Devices, Sunnyvale, CA). *Z*-stacks were acquired with 0.2-µm step size for 6 µm per stack. Camera background noise was measured with each *Z*-stack for normalization during imaging.

Microscopy postprocessing

All fluorescence images were normalized to background noise to account for any variability in camera background signal. To identify cells, 594-nm images were processed by a segmentation script modified from previous work done in our lab (Weir *et al.*, 2017) with binary thresholding instead of canny edge detection. For

aggregates, 488-nm images were processed as previously reported (Weir *et al.*, 2017). For quantifying aggregates in each cell, regions that corresponded to cells in 594-nm images were used to generate masks in the 488-nm images. Previously identified aggregates were then counted within the region of interest of each cell.

Thermotolerance assays

Cells were inoculated into 5 ml of YEP-D and grown overnight at 30°C on a roller drum. The following morning, cells were back-diluted 1:10,000 in fresh media for 12 h before being diluted overnight to OD_{600} < 0.05 in YEP-D. Cells were back-diluted to OD_{600} 0.100 from a log-phase culture and treated with DMSO or 1-NM-PP1. After incubating at 30°C for 3 h, cells were placed on ice for 0-min treatments or 50°C for 30 min. Cells were then placed on ice, diluted in a tenfold series, and spotted onto solid YEP-D. Cells were allowed to grow for 48 h at 30°C before imaging on an Alphaimager (Alpha Innotech, San Leandro, CA).

Doubling time analysis

Cells were grown overnight at room temperature in YEP-D containing 138 µl of glacial acetic acid per 1 l and diluted to OD_{600} = 0.05 the next morning. After 2 h of growth at room temperature, cells were treated with auxin in the form of 3-indoleacetic acid (Sigma) to a final concentration of 500 µM. At 1 h after auxin addition, cells were shifted to the semipermissive temperature of 30°C (*ndc10-1*) or kept at room temperature (all disomic strains), and azetidine 2-carboxylic acid (Sigma) was added to a final concentration of 0.5 mg/ml before measurement of OD_{600} every half hour. The period of exponential growth was used to calculate doubling time using GraphPad Prism software. All OD_{600} measurements were taken using an Ultrospec 2100 *pro* spectrophotometer (Amersham).

Statistical analysis

The statistical tests used are indicated in the figure legends and/or in the *Materials and Methods* or the *Results* section. Values of *n*, definition of center, error bars (e.g., SD and confidence intervals), and significance levels are reported in the figures and/or in the figure legends. All indicated statistical tests were performed using MATLAB, Prism, or R.

ACKNOWLEDGMENTS

We thank members of the Amon and Denic lab for discussions and feedback. We thank Gabriel Neurohr for providing the Bcy1-AID strain. This work was supported by NIH Grants GM127136 to V.D. and CA206157 and GM118066 to A.A., who was an investigator in the Howard Hughes Medical Institute and the Paul F. Glenn Center for Biology of Aging Research at MIT.

REFERENCES

Anckar J, Sistonen L (2011). Regulation of HSF1 function in the heat stress response: implications in aging and disease. Annual review of biochemistry 80, 1089–1115.

Beroukhim R, Mermel CH, Porter D, Wei G, Raychaudhuri S, Donovan J, Barretina J, Boehm JS, Dobson J, Urashima M, *et al.* (2010). The landscape of somatic copy-number alteration across human cancers. Nature 463, 899–905.

Bishop AJ, Louis EJ, Borts RH (2000). Minisatellite variants generated in yeast meiosis involve DNA removal during gene conversion. Genetics 156, 7–20.

Boy-Marcotte E, Perrot M, Bussereau Fo, Boucherie HL, Jacquet M (1998). Msn2p and Msn4p control a large number of genes induced at the diauxic transition which are repressed by cyclic AMP in *Saccharomyces cerevisiae*. J Bacteriol 180, 1044–1052.

Brandman O, Stewart-Ornstein J, Wong D, Larson A, Williams CC, Li G-W, Zhou S, King D, Shen PS, Weibezahn J, *et al.* (2012). A ribosome-bound quality control complex triggers degradation of nascent peptides and signals translation stress. Cell 151, 1042–1054.

Brauer MJ, Huttenhower C, Airoldi EM, Rosenstein R, Matese JC, Gresham D, Boer VM, Troyanskaya OG, Botstein D (2008). Coordination of growth rate, cell cycle, stress response, and metabolic activity in yeast. Mol Biol Cell 19, 352–367.

Brennan CM, Vaites LP, Wells JN, Santaguida S, Paulo JA, Storchova Z, Harper JW, Marsh JA, Amon A (2019). Protein aggregation mediates stoichiometry of protein complexes in aneuploid cells. Genes Dev 33, 1031–1047.

Coote PJ, Jones MV, Seymour IJ, Rowe DL, Ferdinando DP, McArthur AJ, Cole MB (1994). Activity of the plasma membrane H(+)-ATPase is a key physiological determinant of thermotolerance in *Saccharomyces cerevisiae*. Microbiology 140(Pt 8), 1881–1890.

Crawford RA, Pavitt GD (2018). Translational regulation in response to stress in *Saccharomyces cerevisiae*. Yeast 36, 5–21.

Dai C, Whitesell L, Rogers AB, Lindquist S (2007). Heat shock factor 1 is a powerful multifaceted modifier of carcinogenesis. Cell 130, 1005–1018.

Davoli T, Xu AW, Mengwasser KE, Sack LM, Yoon JC, Park PJ, Elledge SJ (2013). Cumulative haploinsufficiency and triplosensitivity drive aneuploidy patterns and shape the cancer genome. Cell 155, 948–962.

Dephoure N, Hwang S, O'Sullivan C, Dodgson SE, Gygi SP, Amon A, Torres EM (2014). Quantitative proteomic analysis reveals posttranslational responses to aneuploidy in yeast. eLife 3, e03023.

Dobson CM (2003). Protein folding and misfolding. Nature 426, 884–890.

Donnelly N, Passerini V, Dürrbaum M, Stingele S, Storchova Z (2014). HSF1 deficiency and impaired HSP90-dependent protein folding are hallmarks of aneuploid human cells. EMBO J 33, 2374–2387.

Gasch AP, Spellman PT, Kao CM, Carmel-Harel O, Eisen MB, Storz G, Botstein D, Brown PO (2000). Genomic expression programs in the response of yeast cells to environmental changes. Mol Biol Cell 11, 4241–4257.

Geiler-Samerotte KA, Dion MF, Budnik BA, Wang SM, Hartl DL, Drummond DA (2011). Misfolded proteins impose a dosage-dependent fitness cost and trigger a cytosolic unfolded protein response in yeast. Proc National Acad Sci 108, 680–685.

Görner W, Durchschlag E, Martinez-Pastor MT, Estruch F, Ammerer G, Hamilton B, Ruis H, Schüller C (1998). Nuclear localization of the C2H2 zinc finger protein Msn2p is regulated by stress and protein kinase A activity. Genes Dev 12, 586–597.

Grably MR, Stanhill A, Tell O, Engelberg D (2002). HSF and Msn2/4p can exclusively or cooperatively activate the yeast HSP104 gene. Mol Microbiol 44, 21–35.

Grimminger-Marquardt V, Lashuel HA (2010). Structure and function of the molecular chaperone Hsp104 from yeast. Biopolymers 93, 252–276.

Guthrie C, Fink GR (1991). Guide to Yeast Genetics and Molecular Biology.

Hartl FU, Bracher A, Hayer-Hartl M (2011). Molecular chaperones in protein folding and proteostasis. Nature 475, 324–332.

Ho Y-H, Gasch AP (2015). Exploiting the yeast stress-activated signaling network to inform on stress biology and disease signaling. Current Genet 61, 503–511.

Hsieh AL, Walton ZE, Altman BJ, Stine ZE, Dang CV (2015). MYC and metabolism on the path to cancer. Seminars Cell Dev Biol 43, 11–21.

Jin X, Moskophidis D, Mivechi NF (2011). Heat shock transcription factor 1 is a key determinant of HCC development by regulating hepatic steatosis and metabolic syndrome. Cell Metabolism 14, 91–103.

Krakowiak J, Zheng X, Patel N, Feder ZA, Anandhakumar J, Valerius K, Gross DS, Khalil AS, Pincus D (2018). Hsf1 and Hsp70 constitute a two-component feedback loop that regulates the yeast heat shock response. eLife 7, e31668.

Kunkel J, Luo X, Capaldi AP (2019). Integrated TORC1 and PKA signaling control the temporal activation of glucose-induced gene expression in yeast. Nat Commun 10, 3558.

Larrimore KE, Barattin-Voynova NS, Reid DW, Ng DTW (2020). Aneuploidy-induced proteotoxic stress can be effectively tolerated without dosage compensation, genetic mutations, or stress responses. Bmc Biol 18, 117.

Longtine MS, McKenzie A, Demarini DJ, Shah NG, Wach A, Brachat A, Philippsen P, Pringle JR (1998). Additional modules for versatile and economical PCR-based gene deletion and modification in *Saccharomyces cerevisiae*. Yeast 14, 953–961.

Oromendia AB, Amon A (2014). Aneuploidy: implications for protein homeostasis and disease. Dis Model Mech 7, 15–20.

Oromendia AB, Dodgson SE, Amon A (2012). Aneuploidy causes proteotoxic stress in yeast. Genes Dev 26, 2696–2708.
Pavelka N, Rancati G, Zhu J, Bradford WD, Saraf A, Florens L, Sanderson BW, Hattem GL, Li R (2010). Aneuploidy confers quantitative proteome changes and phenotypic variation in budding yeast. Nature 468, 321–325.
Santaguida S, Vasile E, White E, Amon A (2015). Aneuploidy-induced cellular stresses limit autophagic degradation. Genes Dev 29, 2010–2021.
Santangelo GM (2006). Glucose signaling in *Saccharomyces cerevisiae*. Microbiol Mol Biol Rev 70, 253–282.
Solís EJ, Pandey JP, Zheng X, Jin DX, Gupta PB, Airoldi EM, Pincus D, Denic V (2016). Defining the essential function of yeast Hsf1 reveals a compact transcriptional program for maintaining eukaryotic proteostasis. Mol Cell 63, 60–71.
Sorger PK, Pelham HR (1987). Purification and characterization of a heat-shock element binding protein from yeast. EMBO J 6, 3035–3041.
Straight AF, Belmont AS, Robinett CC, Murray AW (1996). GFP tagging of budding yeast chromosomes reveals that protein–protein interactions can mediate sister chromatid cohesion. Curr Biol 6, 1599–1608.
Torres EM, Dephoure N, Panneerselvam A, Tucker CM, Whittaker CA, Gygi SP, Dunham MJ, Amon A (2010). Identification of aneuploidy-tolerating mutations. Cell 143, 71–83.
Torres EM, Sokolsky T, Tucker CM, Chan LY, Boselli M, Dunham MJ, Amon A (2007). Effects of aneuploidy on cellular physiology and cell division in haploid yeast. Science 317, 916–924.
Trotter EW, Berenfeld L, Krause SA, Petsko GA, Gray JV (2001). Protein misfolding and temperature up-shift cause G1 arrest via a common mechanism dependent on heat shock factor in *Saccharomycescerevisiae*. PProc Natl Acad Sci USA 98, 7313–7318.
Trotter EW, Kao CMF, Berenfeld L, Botstein D, Petsko GA, Gray JV (2002). Misfolded proteins are competent to mediate a subset of the responses to heat shock in *Saccharomyces cerevisiae*. J Biol Chem 277, 44817–44825.
Weidberg H, Amon A (2018). MitoCPR—A surveillance pathway that protects mitochondria in response to protein import stress. Science 360, eaan4146.
Weir NR, Kamber RA, Martenson JS, Denic V (2017). The AAA protein Msp1 mediates clearance of excess tail-anchored proteins from the peroxisomal membrane. eLife 6, 13004.
Yorimitsu T, Zaman S, Broach JR, Klionsky DJ (2007). Protein kinase A and Sch9 cooperatively regulate induction of autophagy in *Saccharomyces cerevisiae*. Mol Biol Cell 18, 4180–4189.
Zheng X, Krakowiak J, Patel N, Beyzavi A, Ezike J, Khalil AS, Pincus D (2016). Dynamic control of Hsf1 during heat shock by a chaperone switch and phosphorylation. eLife 5, 1153.